RESEARCH

Comparative Methylome Analysis Reveals Epigenetic Signatures Associated with Growth and Shell Color in the Pacific Oyster, *Crassostrea gigas*

Chao Tan[1] · Chenyu Shi[1] · Yin Li[1] · Wen Teng[1] · Yongjing Li[1] · Huiru Fu[1] · Liting Ren[1] · Hong Yu[1,2] · Qi Li[1,2] · Shikai Liu[1,2]

Abstract

Fast growth is one of the most important breeding goals for all economic species such as the Pacific oyster (*Crassostrea gigas*), an aquaculture mollusk with top global production. Although the genetic basis and molecular mechanisms of growth-related traits have been widely investigated in the oyster, the role of DNA methylation involved in growth regulation remains largely unexplored. In this study, we performed a comparative DNA methylome analysis of two selectively bred *C. gigas* strains with contrasted phenotypes in growth and shell color based on whole-genome bisulfite sequencing (WGBS). Genome-wide profiling of DNA methylation at the single-base resolution revealed that DNA methylations were widely spread across the genome with obvious hotspots, coinciding with the distribution of genes and repetitive elements. Higher methylation levels were observed within genic regions compared with intergenic and promoter regions. Comparative analysis of DNA methylation allowed the identification of 339,604 differentially methylated CpG sites (DMCs) clustering in 27,600 differentially methylated regions (DMRs). Functional annotation analysis identified 11,033 genes from DMRs which were enriched in biological processes including cytoskeleton system, cell cycle, signal transduction, and protein biosynthesis. Integrative analysis of methylome and transcriptome profiles revealed a positive correlation between gene expression and DNA methylation within gene-body regions. Protein–protein interaction (PPI) analysis of differentially expressed and methylated genes allowed for the identification of integrin beta-6 (homolog of human ITGB3) as a hub modulator of the PI3K/Akt signaling pathway that was involved in various growth-related processes. This work provided insights into epigenetic regulation of growth in oysters and will be valuable resources for studying DNA methylation in invertebrates.

Keywords DNA methylation · *Crassostrea gigas* · Growth · WGBS · Transcriptional regulation

Chao Tan and Chenyu Shi contributed equally.

✉ Shikai Liu
liushk@ouc.edu.cn

Chao Tan
tanchao@stu.ouc.edu.cn

Chenyu Shi
shichenyu@stu.ouc.edu.cn

Yin Li
liyin1033@stu.ouc.edu.cn

Wen Teng
tengwen@stu.ouc.edu.cn

Yongjing Li
liyongjing@stu.ouc.edu.cn

Huiru Fu
fuhuiru@stu.ouc.edu.cn

Liting Ren
renliting@stu.ouc.edu.cn

Hong Yu
hongyu@ouc.edu.cn

Qi Li
qili66@ouc.edu.cn

[1] Key Laboratory of Mariculture, Ministry of Education College of Fisheries, Ocean University of China, Ocean University of China, 266003 Qingdao, China

[2] Laboratory for Marine Fisheries Science and Food Production Processes, Qingdao National Laboratory for Marine Science and Technology, Qingdao 266237, China

Introduction

The Pacific oyster (*Crassostrea gigas*), as an important aquaculture mollusk, has been widely farmed in many countries around the world (Guo 2009; Troost 2010). With the increasing global demand for *C. gigas*, genetic improvement of production and performance traits becomes crucial to ensure the healthy and sustainable development of the oyster industry. Given its importance, many genetic breeding programs have been carried out for decades. The traits for genetic improvement included but not limited to growth, resistance to pathogens, tolerance to abiotic stressors, and level of nutrients (Azéma et al. 2017; de Melo et al. 2016; Evans and Langdon 2006; Gutierrez et al. 2018; Li et al. 2011), among which growth is one of the most important production traits for improvement in most breeding programs.

Molecular markers have been developed and applied to assist in selective breeding. These included the development of gene-associated single nucleotide polymorphism (SNP) markers that were associated with growth traits (Hu et al. 2021; Li et al. 2011), and the dissection of structural variations (SVs) (Jiao et al. 2021) underlying the genetic basis of growth-related traits in *C. gigas*. Furthermore, fine-scale genetic dissection of growth traits can provide valuable molecular information to guide molecular breeding. Comparative transcriptome analysis of *C. gigas* with contrasted growth performance has been performed to identify a group of genes involved in nucleotide and protein biosynthesis and microtubule activity which may play critical roles in the growth regulation of *C. gigas* (Zhang et al. 2019). With the identification of genes involved in signal transduction pathways that regulate growth in oysters (Kim and Choi 2019; Li et al. 2021), a further question raised is how the transcription of these growth-related genes is regulated. Understanding this aspect should be essential for molecular breeding.

DNA methylation is an important epigenetic modification factor in regulating gene transcription. Epigenetic modification causes heritable changes in gene activity without altering the DNA sequence (Dupont et al. 2009). As an essential epigenetic modification factor, DNA methylation occurs under the catalysis of DNA methyltransferase (DNMT) by attaching the methyl group of S-adenosine methionine (SAM) to the DNA molecule adenine or cytosine for covalent modification (Moore et al. 2013). DNA methylation and demethylation are usually in dynamic balance, while the growth and development will be impaired once the balance is broken. For example, dysregulation of DNA methylation is a defining feature of most cancer types (Baylin and Jones 2016). The role of DNA methylation has been widely demonstrated to have an influence on the phenotypic variation of mammals, especially for the growth trait. The DNA methylation level of insulin-like growth factor 2 (IGF2) in the fetus was positively correlated with birth weight (Bouwland-Both et al. 2013). In addition, DNA methylation has also been demonstrated to affect muscle growth in yak, sheep, chicken, and other species with economic importance (Fan et al. 2020; Hu et al. 2013; Ma et al. 2019). In the study of DNA methylation in pigs with different body sizes, it was found that differentially methylated genes (DMGs) were mainly enriched in lipid metabolism and muscle development, suggesting that DNA methylation may affect the tendency of obesity and body size by regulating gene expression in skeletal muscle (Yang et al. 2017). In invertebrates, previous studies have shown that their genomes were far less methylated than those of vertebrates with DNA methylation predominantly present in gene-body regions (Gavery and Roberts 2013; Suzuki et al. 2007). These methylation patterns in invertebrates may be necessary for facilitating phenotypic variation, contributing to the increased adaptive potential (Roberts and Gavery 2012). Recent studies have revealed that DNA methylation was crucial for early development), shell formation (Zhang et al. 2020), and regulation of adaptation to environmental changes (Wang et al. 2021) in bivalves.

Numerous methods have been developed to profile DNA methylation at the genome level. One of the most widely used is whole-genome bisulfite sequencing (WGBS) (Wang 2013). The core of this method is to treat DNA with bisulfite followed by whole-genome sequencing. The unmethylated cytosine is converted into uracil, while the methylated cytosine remains, allowing for identifying methylated cytosine sites after DNA sequencing. The conversion process is critical for the success of WGBS, which includes three major steps (Esteller 2005). Cytosine first reacts with $NaHSO_3$ to form sulfonated cytosine (cytosine-SO_3) derivatives. Then sulfonated cytosine derivatives undergo hydrolysis and deamination to form sulfonated uracil (uracil-SO_3) derivatives. Lastly, the sulfonated uracil derivatives are treated with alkali to remove the sulfonic acid group to form uracil, while the 5-methylcytosine in the DNA remains unchanged. Therefore, bisulfite treatment of genome DNA followed by high-throughput sequencing allows for genome-wide DNA methylation profiling at single-base resolution.

In this study, we performed a comparative DNA methylation analysis of two *C. gigas* strains with contrasted phenotypes in growth and shell color using WGBS. We first developed genome-wide DNA methylation profiles for the two strains, then compared them to detect differentially methylated regions for the identification of differentially methylated genes. Finally, integrative analysis of DNA methylome and transcriptome was performed to explore the regulatory

role of DNA methylation in gene expression involved in the growth of the oyster. This work generated valuable resources for the study of DNA methylation in invertebrates and provided insights into epigenetic regulation of growth in oysters.

Materials and Methods

Experiment Animals and Sample Collection

The animals used for this work were from two full-sib families of *C. gigas* constructed in June 2018. The parents for one full-sib family were from a fast-growing strain (hereinafter referred to as HH) which has been selected for growth for over ten generations, while the parents for the other full-sib family were from a slow-growing strain (hereinafter referred to as CC) which was a highly inbred line produced through generations of inbreeding. The rearing of larvae and spats was maintained the same for both families. In September 2018, the 3-month-old individuals from the fast-growing family (HH, average shell height of 18.60 ± 0.21 mm) and the slow-growing family (CC, average shell height of 14.20 ± 0.19 mm) were collected. Three oysters from each family were randomly selected for dissection of whole soft tissues, which were used as three biological replicates in this study. The tissues were flash-frozen in liquid nitrogen and kept in -80 ℃ freezer until use. All animal care and use procedures were approved by the Institutional Animal Care and Use Committee of Ocean University of China (Permit Number: 20141201) and were performed according to the Chinese Guidelines for the Care and Use of Laboratory Animals (GB/T 35,892–2018).

DNA Extraction, Library Construction, and Sequencing

The soft tissues of the oyster were thoroughly grounded, followed by genomic DNA extraction using the improved phenol–chloroform method (Li et al. 2006). The purity of genomic DNA was tested using NanoPhotometer® spectrophotometer (IMPLEN, CA, USA). The concentration of genomic DNA was determined using Qubit® DNA Assay Kit in Qubit® 2.0 Fluorometer (Life Technologies, CA, USA). For methylation analysis using whole-genome bisulfite sequencing, 26 ng lambda DNA was added to the genomic DNA to test bisulfite conversion efficiency. Genomic DNA was fragmented to 200–300 bp using ultrasound, followed by terminal remediation and adenylation, and then the methylated cytosine barcode was connected to the DNA fragments. Genomic DNA fragments were treated twice with bisulfite using EZ DNA Methylation-Gold™ Kit (Zymo Research) and then amplified by PCR using KAPA

HiFi HotStart Uracil + ReadyMix ($2 \times$). Qubit® 2.0 Fluorometer (Life Technologies, CA, USA) and quantitative PCR were used to quantify the concentration of the libraries. Agilent Bioanalyzer 2100 system was used to detect the insert size. A total of six libraries were constructed and were sequenced using Illumina NovaSeq 6000 for 150-bp paired-end reads.

Read Quality Control and Mapping

The FastQC program (Brown et al. 2017) was used for quality control of the raw reads generated from the sequencer. Then, the Trimmomatic software (Bolger et al. 2014) with main parameters (SLIDINGWINDOW: 4:15; LEADING:3; TRAILING:3; ILLUMINACLIP: adapter.fa: 2:30:10; MINLEN:36) was used to filter the adapters and low-quality data. The clean reads were mapped to *C. gigas* reference genome (Assembly: GCA_902806645.1, cgigas_uk_roslin_v1) using BSMAP software (Xi and Li 2009) with parameters (-R -p 4 -n 1 -r 0 -S 1). The R package RIdeogram (Hao et al. 2020) was used to visualize the DMRs density and marked genes on a genome-wide scale. The clusterSamples and getCorrelation commands of the R package methylKit (Akalin et al. 2012) were used to perform Pearson correlation analysis and sample clustering analysis based on CpG DNA methylation of CC and HH strains.

Methylation Calling and Identification of Differentially Methylation Regions

The MCALL module in MOABS (Sun et al. 2014) was used to call DNA methylation with default parameters. The percentage of cytosine sequenced to the reference cytosine of the lambda genome was used to assess the bisulfite conversion rate. Then, the MCOMP module in MOABS was used to identify differentially methylated CpG sites (DMCs) and differentially methylated regions (DMRs). In this study, only methylated C sites with more than $3 \times$ sequence coverage were used for differential analysis. The credible methylation difference (CDIF) value greater than 0.2 was considered DMC. The DMR was defined as the region containing at least three DMCs, with the differential methylation more than 0.2 and the *p*-value from Fisher's exact test less than 0.05. The putative promoter regions were defined as 2 kb upstream of the TSS.

SNP Identification and Correlation Analysis

SNP calling was conducted using CGmapTools software (Guo et al. 2018). High-quality SNPs were filtered from positions with coverage of $10 \times -100 \times$. The VCF SNP datasets were used to calculate *p*-distance between individuals using VCF2Dis (https://github.com/BGI-shenzhen/VCF2D

is). To assess the genetic effect on the epigenetic difference between CC and HH strains, the Fst for each SNP between the two strains was calculated (Bhatia et al. 2013), and a correlation analysis of gene averaged Fst with methylation levels was performed according to the method previously reported (Liew et al. 2020). In order to remove the bias caused by few SNPs or methylation sites, we only analyzed genes with the number of CpG sites ≥ 5 and SNPs ≥ 10.

Functional Annotation of Differentially Methylated Genes

The differentially methylated genes (DMGs) were annotated from the DMRs based on the genome annotation file. DMGs were identified as genes whose gene body region or promoter region had at least 1-bp overlap with the DMRs. To understand the function of the DMGs, we obtained functional annotations of the *C. gigas* protein-coding genes by integrating the blast results from three different databases, including NCBI non-redundant (nr) protein database, Egg-NOG, and BlastKOALA. The ClusterProfiler (Yu et al. 2012) R package was used for GO and KEGG enrichment analysis and the result with a p-adj < 0.05 were considered significantly enriched.

Integrative Analysis of DNA Methylation with Gene Expression

To investigate the connection between DNA methylome and transcriptome, we performed an integrative analysis of DNA methylation with the transcriptome profiles that was determined by RNA-seq of the same samples (Shi et al. 2022). The Pearson correlation coefficient (r) was performed to assess the correlation between the gene body DNA methylation and gene expression levels (expression gene, FPKM > 0.1) on a genome-wide scale. Further, we divided all protein-coding genes into non-expression genes (FPKM < 0.1) and expression genes (FPKM > 0.1). The expression genes were then further divided into three groups, including the first quartile of low-expression genes,

the last quartile of high-expression genes, and the rest of the medium-expression genes. We also performed an integrated analysis of LncRNA and DNA methylation.

To systematically identify hub genes from the DEGs that were significantly associated with the phenotypic differences, we first built the protein–protein interaction (PPI) networks according to the STRING database, followed by the construction of a gene interaction subnet by mapping the DEGs onto the PPI network. As the maximal clique centrality (MCC) algorithm has a better performance on the precision of predicting essential proteins from the PPI network (Chin et al. 2014), we screened the hub genes in the PPI network according to the MCC scores by cytoHubba in Cytoscape. Given a node v, the MCC of v is defined as $MCC(v) = \sum_{C \in S(v)}(|C| - 1)!$, where $S(v)$ is the collection of maximal cliques which contain v, and $(|C| - 1)!$ is the product of all positive integers less than $|C|$. In this study, the genes with the top 10 MCC scores were considered hub genes. The levels of both expression and DNA methylation of the hub genes were visualized by using an integrative genomics viewer (IGV).

Results

DNA Methylation Pattern of Two Oyster Strains

Whole-genome bisulfite sequencing generated 176.1 million reads with 158.49 Gb for the six samples. After trimming, 143.56-Gb clean reads were obtained for downstream analysis. Mapping of the clean reads against the oyster reference genome assembly showed an average mapping rate of 51.72%, ranging from 48.44 to 52.59%. Assessment of the bisulfite treatment efficiency using the lambda genome suggested high levels of the bisulfite conversion rate of over 99.3% for all the samples (Table 1). The global DNA methylation profiles showed significant differences in the mean methylation ratio of C (mC) between the two strains ($P < 0.05$), though the mean DNA methylation ratio of CpG, CHH, and CHG was not significantly different (CpG: $P = 0.204$; CHG: $P = 0.404$; CHH: $P = 0.260$). Classification

Table 1 Summary of whole genome bisulfite sequencing and read mapping to the *C. gigas* genome

Sample ID	Raw reads (million)	Clean reads (million)	Clean bases (Gb)	Mapped reads (million)	Mapped rate (%)	Bisulfite conversion rate (%)
CC1	181.31	178.99	24.71	93.09	52.01	99.48
CC2	172.82	170.46	23.50	89.60	52.57	99.47
CC3	179.44	177.03	24.41	85.74	48.44	99.36
HH1	150.56	148.46	20.50	77.59	52.27	99.47
HH2	194.84	191.12	26.37	100.25	52.46	99.46
HH3	177.63	174.43	24.07	91.73	52.59	99.47

Table 2 Mean methylation ratio (mean ratio) of C, CpG, CHG, CHH

Sample ID	Context	Methylation level (%)
CC1	C	1.40
	CpG	12.62
	CHG	0.45
	CHH	0.55
CC2	C	1.41
	CpG	12.51
	CHG	0.46
	CHH	0.56
CC3	C	1.43
	CpG	12.06
	CHG	0.51
	CHH	0.62
HH1	C	1.39
	CpG	12.10
	CHG	0.47
	CHH	0.55
HH2	C	1.38
	CpG	12.11
	CHG	0.48
	CHH	0.57
HH3	C	1.37
	CpG	12.03
	CHG	0.46
	CHH	0.56

for each type of mC contexts (i.e., CpG, CHG, or CHH) showed that the mCpG was the most frequently occurring methylation, followed by mCHHs and mCHGs (Table 2). The results suggested that mCpG was the primary type of DNA methylation in the oyster, which was consistent with previous reports (Wang et al. 2021). Therefore, we mainly focused on the methylation within CpG motifs in the downstream analysis.

Sample clustering based on DNA methylation profiles showed that the six samples were clustered into two groups, CC and HH (Fig. 1a). The Pearson correlation analysis of CpG DNA methylation suggested a high level of reproducibility among the samples within the group, while a significant difference between the two groups (Fig. 1b). Distribution of DNA methylation across the genome revealed a relatively wide distribution but with obvious hotspots within chromosomes and significant difference among chromosomes (Fig. 2a). For instance, within most chromosomes, higher levels of DNA methylation were observed around the center of the chromosome (Fig. 2a). Notably, chromosomal regions with high levels of DNA methylation corresponded to regions with a high density of repeats (Fig. 2a). Comparison of the mean methylation ratio of each chromosome

suggested variations in methylation level across chromosomes, with the lowest level in chromosome 2 which had low gene density (Fig. 2a, b). The DNA methylation levels in genic and intergenic regions were compared as shown in Fig. 2c. Apparently, higher methylation levels were present in genic regions than in intergenic regions (Fig. 2c). The patterns of DNA methylation within genes were similar in both strains, but a significant difference in CpG DNA methylation level was observed in intergenic regions between CC and HH strain (Fig. 2c), while within genes, the CpG methylation levels of gene body regions were significantly different from that of 2-kb upstream and downstream regions with a significantly higher methylation level being observed within the gene-body regions (Fig. 2d). In contrast, the patterns of CHG and CHH methylations within gene body and its up- and downstream were different from that of CpG methylation with no significant difference being observed between gene body and 2-kb up- and downstream regions. Furthermore, we found that levels of DNA methylation were variable among the four major types of DNA repetitive elements, with higher levels in DNA transposons and SINE, while lower levels in LTR and LINE. Notably, a significant difference in DNA methylation levels between CC and HH strains was observed in LTRs (Fig. 2e).

Estimation of Genotypic Effect on Methylation Diversity

We obtained an average of 2,212,518 and 2,326,532 SNPs from the WGBS data of the CC and HH strains, respectively. Although the number of SNPs in the HH strain was slightly higher than that in the CC, there was no significant difference ($P = 0.30$). We also analyzed the distribution of SNP types, and we found no significant differences in all types of SNPs between the two strains, especially the $C > T$ SNPs that could be misidentified as unmethylated CpG after bisulfite conversion of DNA (Fig. 3a). Therefore, we speculate that the SNP data will not affect the analysis of WGBS.

Pairwise p-distance analysis showed that oysters from the same strains were clustered, indicating that they were more genetically similar (Fig. 3b). The correlation analysis of Fst with DNA methylation differences between the CC and HH strains showed that there was a very weak correlation in the gene body ($r = -0.0081$) and exon ($R = -0.0041$) regions (Fig. 3c, d). This indicated that the epigenetic diversity we detected in CC and HH strains was independent of genotype.

Identification of DMCs and DMRs Between Two Oyster Strains

A total of 9,110,189 CpG sites were identified from both CC and HH strains. To investigate the difference in DNA methylation profile, we identified the differentially
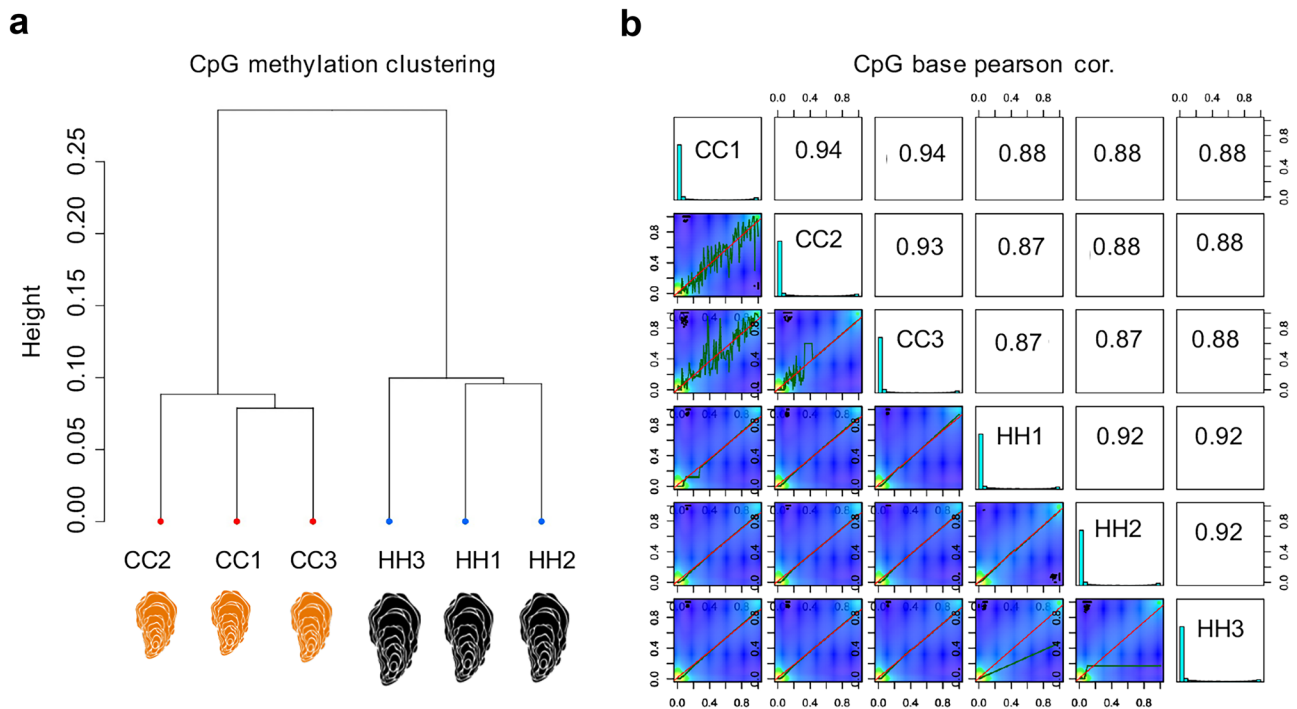
a

CpG methylation clustering

b

CpG base pearson cor.

Fig. 1 Sample clustering. **a** Clustering of CpG methylation among samples. **b** The Pearson correlation coefficients of CpG methylation among samples

methylated CpG sites (DMCs) and differentially methylated regions (DMRs) between the two strains, HH and CC. A total of 159,831 CpG sites were methylated at higher levels in HH strain than CC strain (hereafter referred to as hyper DMC), and a total of 179,773 CpG sites were methylated at lower levels in HH strain than CC strain (hereafter referred to as hypo DMC) (Table S1). Interestingly, the DMCs were mainly enriched in intronic regions, followed by exons, intergenic regions, and promoter regions (Fig. 4a). In total, 27,600 DMRs were identified, including 12,692 hyper and 14,908 hypo DMRs (Table S2), showing drastic differences in methylation levels between HH and CC strains (Fig. 4b, c). Together, the total size of DMRs was 7,647,143 bp, accounting for 1.18% of the whole genome. Besides, a higher density of DMRs was observed around the center of most chromosomes (Fig. 4d). Meanwhile, some of the growth-related genes reported in previous QTL mapping or GWAS studies (He et al. 2021; Wang 2018) were located in DMRs, such as TRMT12 (LOC105332610), P3H2 (LOC105325684), and CFAP61 (LOC105320109) (Table S2). Furthermore, several previously reported genes associated with shell color (Han et al. 2021; Wang 2018), including sucD (LOC105319941), EXOSC10 (LOC105330593), TUB-GCP4 (LOC105330131), TRIM45 (LOC117680499), and TNKS (LOC105342415), were also located DMRs identified between the two strains (Table S3).

Identification and Functional Enrichment Analysis of DMGs

Based on genome annotation, we identified a total of 11,033 DMGs from the DMRs between CC and HH strains. Functional analyses of these genes were performed based on their enrichment in the GO and KEGG databases. GO enrichment analyses revealed that DMGs were enriched in a total of 108 GO terms (p-adj < 0.05; Table S3),many of which were associated with the cytoskeleton system, such as microtubule-based movement (GO:0,007,018), microtubule (GO:0,005,874), dynein complex (GO:0,030,286), microtubule motor activity (GO:0,003,777), structural constituent of cytoskeleton (GO:0,005,200), and kinesin complex (GO:0,005,871) (Fig. 5a, Table S4). DMGs were also enriched in GO terms related to cell cycle, including cell cycle (GO:0,007,049), cell division (GO:0,051,303), regulation of G2/M transition of the mitotic cell cycle (GO:0,010,389), and cyclin-dependent protein serine/threonine kinase activity (GO:0,004,693) (Fig. 5a, Table S4). Some of DMGs were enriched in GO terms related to the signal transduction process such as GTPase activator activity (GO:0,005,096), protein serine/threonine kinase activity (GO:0,004,674), and protein phosphorylation (GO:0,006,468). Meanwhile, many of the DMGs were enriched in transcription and translation-related terms, such as RNA export from the nucleus (GO:0,006,405 and GO:0,006,406), tRNA binding (GO:0,000,049), ribosome

Fig. 2 DNA methylation landscape across the genome and within protein-coding genes. **a** Distribution of CpG DNA methylation across the genome of *C. gigas*. **b** Comparison of mean DNA methylation ratio of CC and HH groups among chromosomes. **c** Comparison of mean DNA methylation ratio between CC and HH groups in genic and intergenic regions. Asterisks indicate significant differences. **d** DNA methylation profiles of gene body, 2 kb upstream of transcription start site (TSS) and 2 kb downstream of transcription end site (TES). **e** Comparison of mean DNA methylation ratio of CC and HH groups in transposable elements of DNA transposon, LTR, SINE, and LINE. Asterisks indicate significant differences
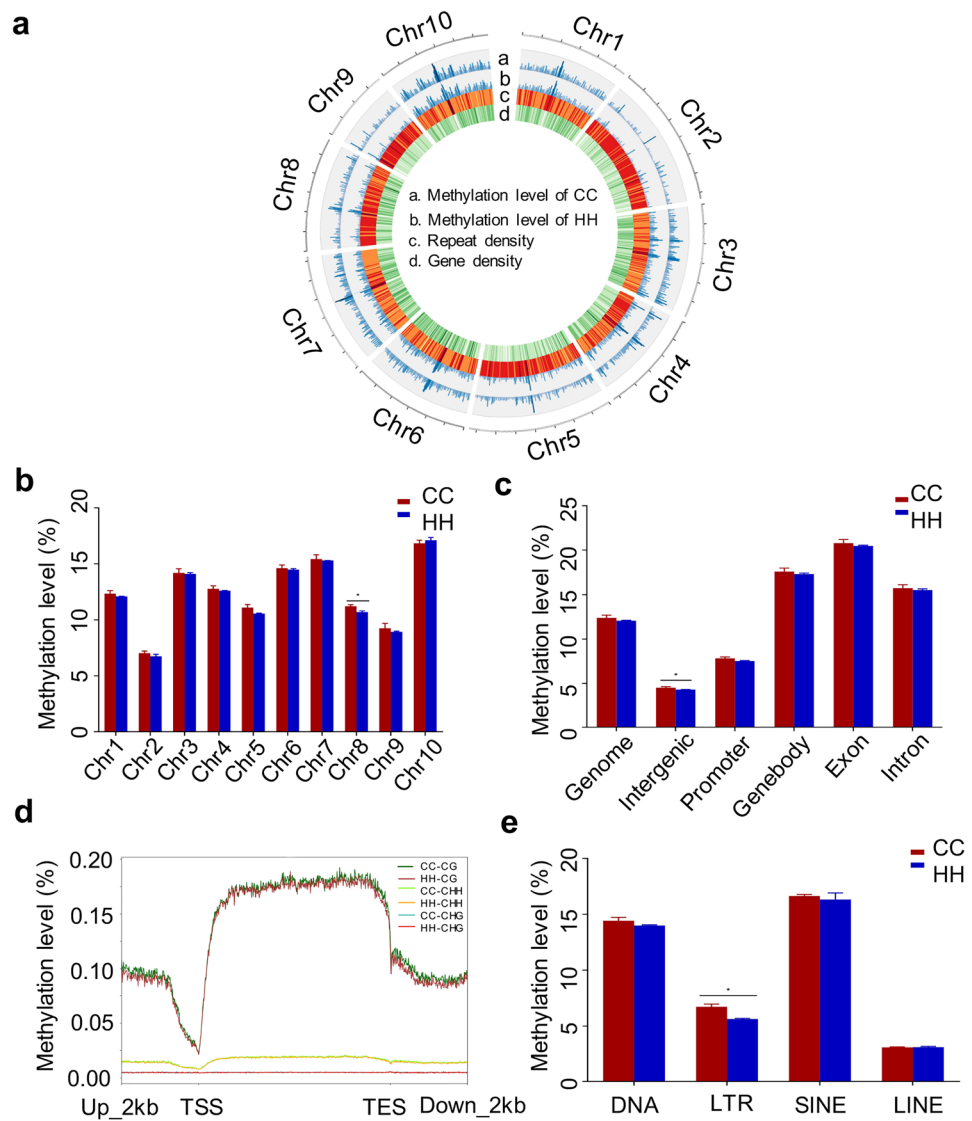
biogenesis (GO:0,042,254), transcription corepressor activity (GO:0,003,714), and snRNA transcription by RNA polymerase II (GO:0,042,795) (Fig. 5a, Table S4).

KEGG pathway analysis showed that the DMGs were significantly enriched in 23 KEGG pathways. Among these 23 pathways, eight pathways were related to transcription and translation, such as RNA transport (ko03013), ribosome biogenesis (ko03009), spliceosome (ko03040 and ko03041), transfer RNA biogenesis (ko03016), transcription machinery (ko03021), protein processing in the endoplasmic reticulum (ko04141), and ribosome biogenesis in eukaryotes (ko03008) (Fig. 5b and Table S5). DMGs were also enriched in KEGG pathways related to the signal transduction process such as ABC transporters (ko02010), oxidative phosphorylation (ko00190), and inositol phosphate metabolism (ko00562). Meanwhile, many of the DMGs also enriched in DNA repair and recombination proteins (ko03400), cell

cycle (ko04110 and ko04111), and cytoskeleton proteins (ko04812) (Fig. 5b and Table S5).

Integrative Analysis of DNA Methylation and Transcriptome Profiles

To understand the role of DNA methylation in regulating gene transcription, we integrated the methylation profiling with analysis of RNA-seq data generated from the same samples to investigate the correlation between DNA methylation and gene expression at a genome-wide scale. Overall, the level of methylation within the gene body was positively correlated with the level of gene expression in the oyster (Fig. 6a, b). Significantly, the higher the level of gene expression was, the higher the level of methylation was observed, especially within gene-body regions (Fig. 6c, d). Similar patterns of correlation between methylation and

Fig. 3 Assessment of genetic effect on DNA methylation. **a** Distribution of single nucleotide polymorphisms (SNPs) in CC and HH WGBS libraries. **b** Pairwise *p*-distance analysis and clustering of SNP data from all 6 samples. **c** Scatterplot of *F*st values and methylation-level difference in the gene body of CC and HH strains. **d** Scatterplot of *F*st values and methylation-level difference in exon region of CC and HH strains
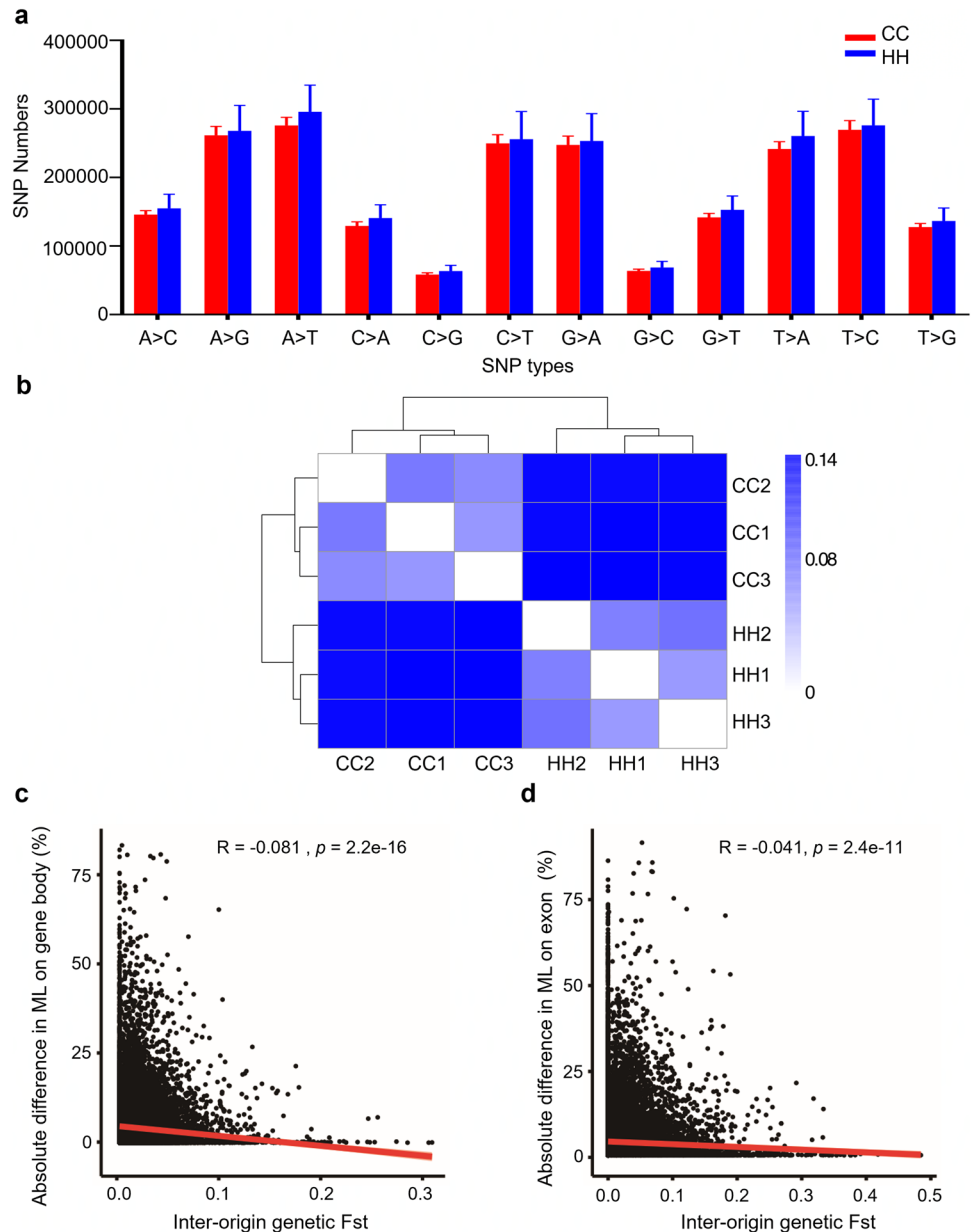

gene expression were observed in both CC and HH strains (Fig. 6).

To further determine the relationship of gene expression with regulation by DNA methylation, we focused on the differentially expressed genes (DEGs) and differentially methylated genes (DMGs) between CC and HH strains. A total of 2133 genes were both DEGs and DMGs identified from the two strains. Of which, 1820 DEGs were differentially methylated within the gene-body regions (gene body-DMGs-DEGs), while 580 DEGs were differentially methylated in the promoter regions (promoter-DMGs-DEGs) (Table S6). Further analysis of 1,820 gene body-DMGs-DEGs) showed that 985 genes (54.12%) showed a positive correlation between methylation and

gene expression (Fig. 7a). Of the 580 promoter-DMGs-DEGs, 274 genes showed a negative correlation between methylation and gene expression (Fig. 7b). The hub genes, screened from the network using the maximal clique centrality (MCC) method, were mostly related to DNA replication, cell adhesion, and cellular metabolic process (Table S7). Further analysis of these genes allowed for the identification of a critical gene related to growth, integrin beta-6 (LOC105346726), which was the homolog of human ITGB3 (Fig. 7c). Significantly, compared to HH strain, the promoter region of integrin beta-6 gene showed a higher level of DNA methylation in CC strain (fold change was 2586.20), corresponding to the extremely low level of expression (fold change was 11.78) (Fig. 7d and Table S7).

Fig. 4 Identification of differentially methylated CpG sites and regions between CC and HH strains. **a** The number of differentially methylated CpG sites (DMCs) within different genomic functional regions. The hyper DMCs indicate higher methylation levels in HH compared with CC strain, while hypo DMCs indicate lower methylation levels in HH compared with CC strain. **b** Heatmap of methylation levels within DMRs identified between CC and HH strains. **c** The number of differentially methylated regions (DMRs) identified in each chromosome. **d** Distribution of DMRs and previously reported genes associated with growth and shell color in chromosomes. The green squares indicate genes associated with growth-related traits (Wang 2018; He et al. 2021). Black circles indicate genes associated with shell black color (Wang 2018). The orange circles indicate genes associated with shell orange color (Han et al. 2021)
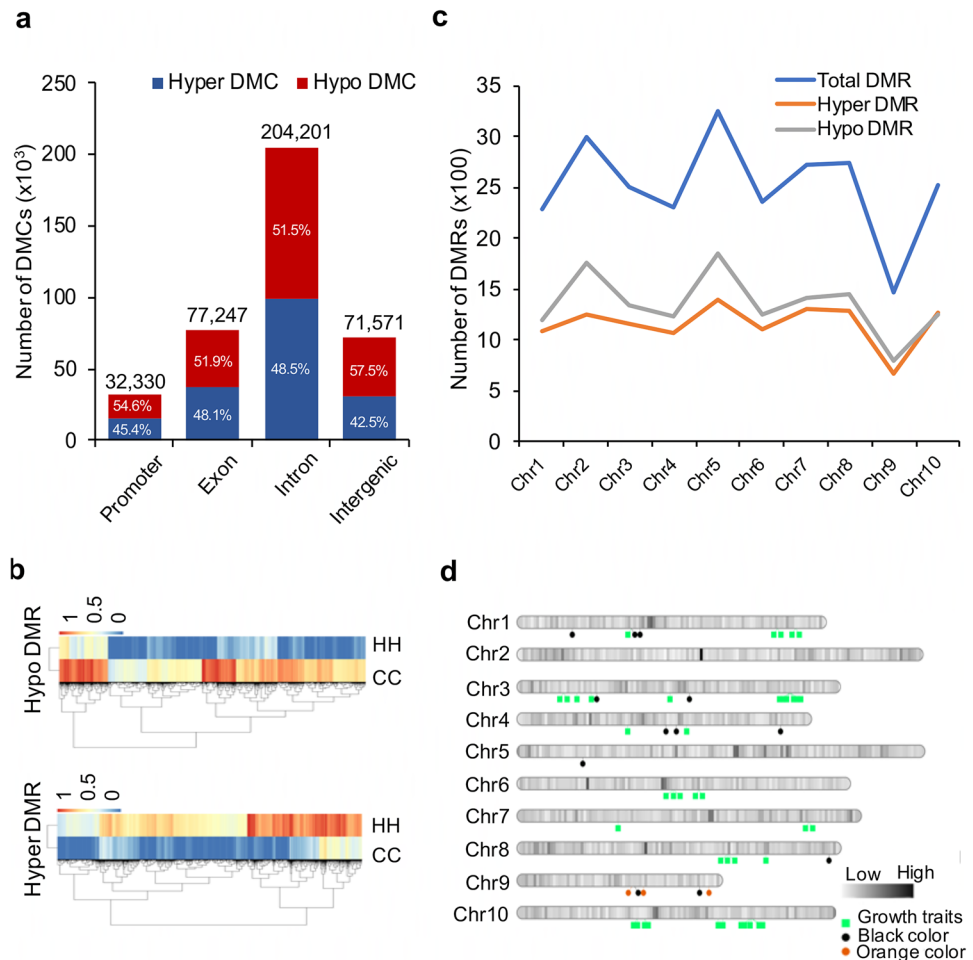
The relationship between LncRNA expression and DNA methylation was further explored. By integrating the expression of LncRNA with DNA methylation within the gene body and promoter, we found that neither gene body DNA methylation nor promoter DNA methylation showed a significant correlation with LncRNA expression (CC gene body: $R=0.03$; CC promoter: $R=0.062$; HH gene body:0.021; HH promoter: 0.026) (Fig. 8). Among the 2,676 differentially expressed lncRNAs (DELncRNAs), only 655 DELncRNAs overlapped with DMRs, of which 198 lncRNAs had DMRs in their promoters, while 568 lncRNAs had DMRs in the gene body (Table S8).

Discussion

A better understanding of the genetic basis and molecular mechanisms involved in transcriptional regulation of production and performance traits is essential for molecular breeding. DNA methylation is one of the well-recognized epigenetic modifications involved in transcriptional regulation to affect phenotypic plasticity in various organisms (Fan et al. 2020; Hu et al. 2013; Ma et al. 2019). In this work, we performed a comparative analysis of the DNA methylome of the two *C. gigas* strains with contrasted growth performance to explore the regulatory mechanism of DNA methylation in the growth of *C. gigas*. Based on the CpG methylation, the samples were clustered well into two groups suggesting the distinct methylation profiles of the two oyster strains. Firstly, we investigated DNA methylation patterns in *C. gigas* by developing genome-wide DNA methylation profile. At the chromosomal level, DNA methylation occurred mainly around the center of chromosomes. At the gene level, exonic regions showed the highest DNA methylation levels. The differentially methylated CpG sites were mainly present in intronic regions. Furthermore, DMR-related genes were annotated from DMRs to better understand the potential mechanism of DNA methylation regulation of growth in *C. gigas*. Finally, through integrative analysis of DNA methylome and transcriptome, we found that DNA methylation was positively correlated with gene expression within gene body regions. Protein–protein interaction (PPI) analysis of differentially expressed and methylated genes revealed that the integrin beta-6 (homolog of human ITGB3), as a hub
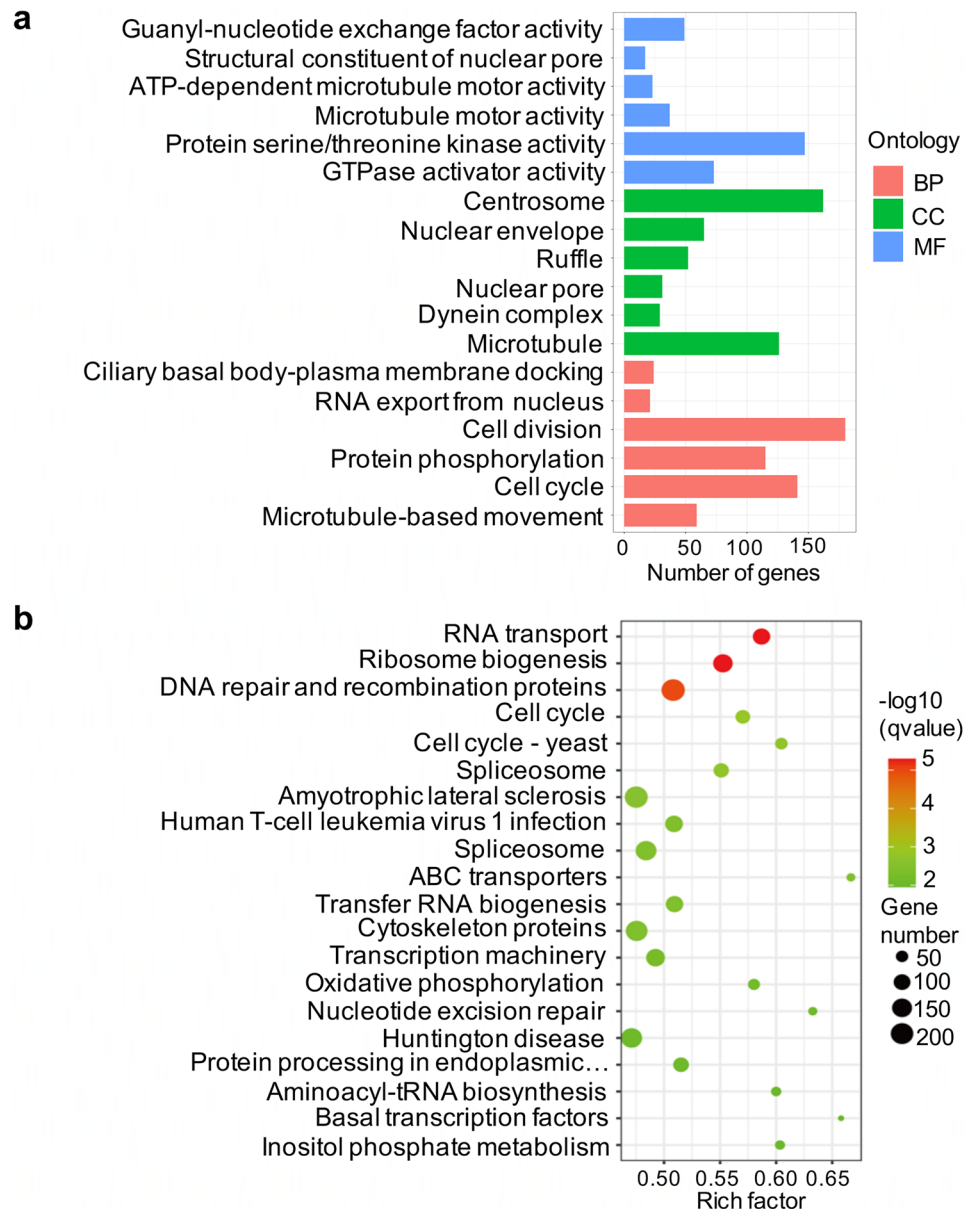
modulator of the PI3K/Akt signaling pathway, could be critical in growth regulation in the *C. gigas*.

With the high-quality genome assembly and annotation data, we compared the distribution of DNA methylation with repetitive elements and genes across the *C. gigas* genome. As previously reported, the DNA methylation is of mosaic type in mollusks, with stretches of hypermethylated DNA alternating with hypomethylated stretches (Männer et al. 2021). Notably, we found that for most chromosomes, a high rate of DNA methylation was always observed in the center region of chromosomes, where a high density of repetitive sequences was present. Numerous studies have proven that (peri)centromeres were characterized by DNA

hypermethylation and enrichment in repetitive sequences (Achrem et al. 2020; Scelfo and Fachinetti 2019). Based on this, our result may suggest the putative location of centromeres within chromosomes in the oyster.

Repetitive DNA elements (REs), as the most abundant type of sequence in the genome, account for the majority of methylated sites in the genome (Pappalardo and Barra 2021). Recent studies clearly show that methylation processes that shape repetitive genome compartments of bivalve mollusks are nonrandom, quite complex, and not necessarily uniform (Šatović Vukšić and Plohl 2021). Consistently, in this work, we observed different levels of methylation among four basic transposable elements (TEs) (Wells and Feschotte 2020), of

Fig. 6 Integrative analysis of DNA methylome and transcriptome. **a**, **b** Correlation analysis of DNA methylation in the gene body and gene expression in CC and HH strains. **c**, **d** Distribution of methylation levels within protein-coding genes with different expression levels (non-expression genes: FPKM < 0.1; expression genes: FPKM > 0.1) in CC and HH strains
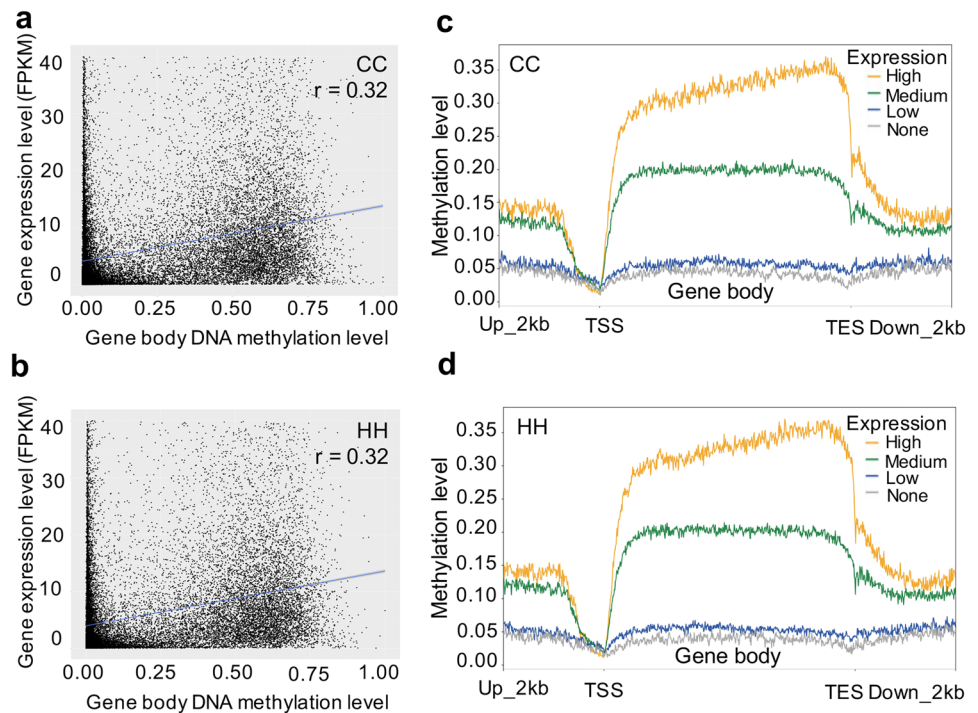

which a significantly different level of methylation in the type of LTR repeats was observed between the two strains. The LTR repeats contain abundant transcriptional regulatory signals such as enhancers and promoters (Cohen et al. 2009). Hypermethylation of LTRs can significantly reduce the binding affinities of the enhancer motifs to the key transcription factors that suppress transcription (Hu et al. 2017), which may play important roles in genomic diversity and phenotypic variations.

The occurrence of DNA methylation is variable across chromosomes, with the lowest DNA methylation rate being observed in chromosome 2, which is generally consistent with the density of genes. DNA methylation in the oyster tended to occur in genic regions, which was consistent with observations in previous studies (Wang et al. 2021). Within genes, exonic regions showed higher levels of DNA methylation than intronic regions. However, the DMCs identified between the two oyster strains through comparative methylation analysis were mainly from intronic regions (60.13%). The DNA methylation present within gene-body regions might alter chromatin structure and affect transcription elongation efficiency (Tunjić-Cvitanić et al. 2021). Studies have reported that methylated genes have a higher degree of conservation across species than unmethylated genes, and genes containing introns were more likely to be methylated than those lacking introns (Gavery and Roberts 2010; Lyko et al. 2010). Previous studies have shown that DNA methylation of the first intron tended to be negatively correlated with

gene expression across various tissues and species (Anastasiadi et al. 2018). Combined with the abovementioned observations, it is speculated that the DMCs enriched in introns as observed in this work may also have vital functions in fine-tuning gene expression in the oyster.

Significant differences in DNA methylation profiles were observed between CC and HH strains. The mean methylation ratio of C was significantly higher in the CC strain than that of HH ($p < 0.05$). Studies have shown that DNA methylation increased in the offspring with inbreeding depression (Vergeer et al. 2012). Therefore, the high DNA methylation levels in the slow-growing CC strains observed in the present study could be associated with inbreeding. Methylations associated with growth and shell color were inferred from genes with differential methylation between the two strains showing contrasted phenotypes in growth and shell color. Growth is a complex trait regulated by a complicated network of genes and pathways. Enrichment analysis of DMGs allowed for the identification of biological processes including cytoskeleton system, cell cycle, signal transduction process, protein transcription, and translation, which were reported to play critical roles in growth regulation. The cytoskeleton plays an important role in maintaining cell shape and the stability of the intracellular structure, which is involved in various biological activities, including cellular material transport, formation of the muscle cell power system, and separation of chromosomes in cell division (Julicher et al. 2007; Park et al. 2020;

Fig. 7 Gene-body, promoter DNA methylation with gene expression. **a** Correlation of differential methylation in the gene body and differential gene expression identified between CC and HH strains. **b** Correlation of differential methylation in promoter and differential gene expression identified between CC and HH strains. **c** The protein–protein interaction (PPI) networks of differentially expressed genes between CC and HH strains. The PPI networks were developed based on human homologs. The filled color of ellipses indicates the degree of interaction. **d** Visualizations of methylation (WGBS) and expression (RNAseq) between CC and HH strains for integrin beta-6, the homolog of human ITGB3. The green line represents the gene body, and the red line represents the upstream 2 kb of the gene body
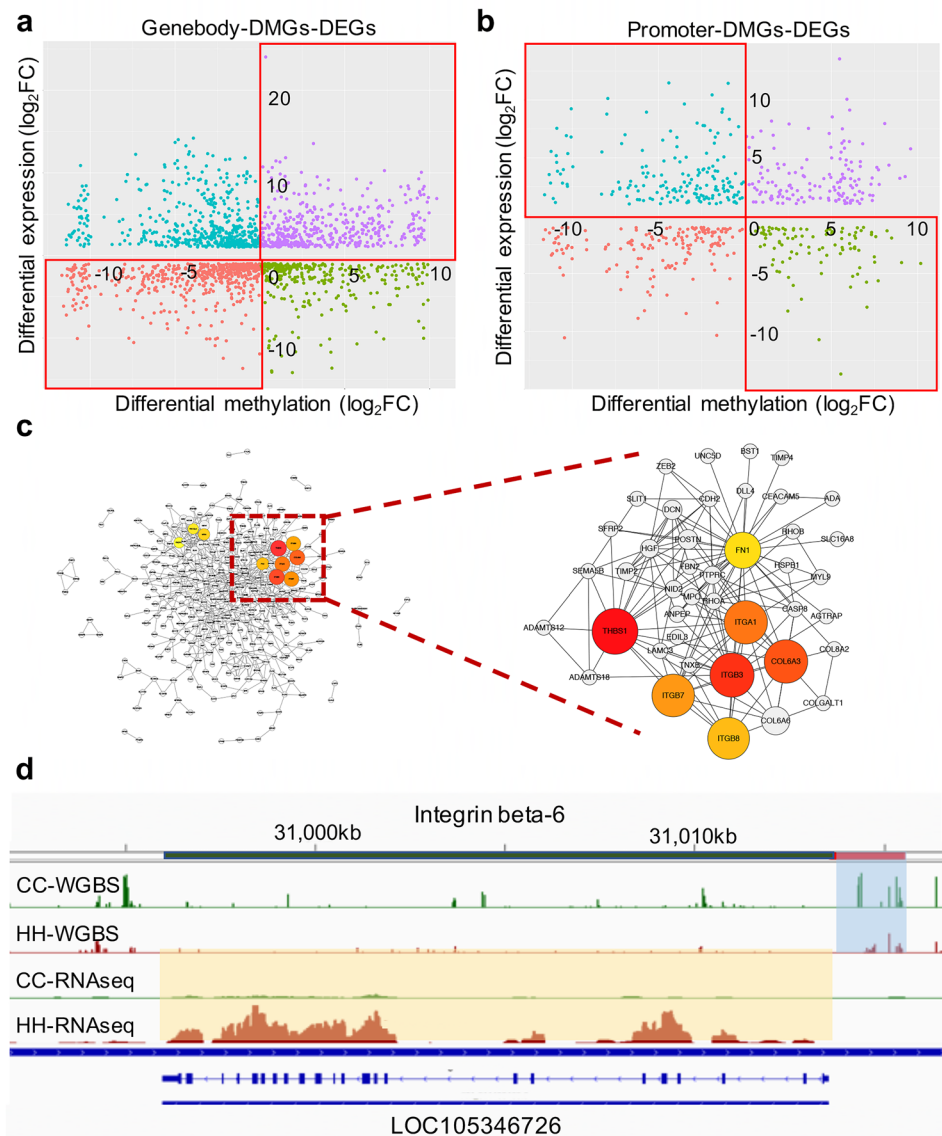
Wickstead and Gull 2011). The cell cycle, also known as the cell proliferation phase, is involved in the whole process of organism growth and development by maintaining tissue homeostasis (Pucci et al. 2000; Vermeulen et al. 2003). Signal transduction is the process by which chemical or physical signaling molecules are transmitted to cells, eventually leading to cellular reactions, and is the basic mechanism that controls cell growth, proliferation, and metabolism (Krauss 2003). Integrative analysis with QTL mapping for shell color in *C. gigas* revealed that the genes associated with the black color (sucD, EXOSC10, TUBGCP4), and the orange color (TRIM45, and TNKS) (Han et al. 2021; Wang 2018) showed significant differences in DNA methylation between the CC and HH strains in this study. This provided valuable resource for further studies on molecular mechanism of shell color in *C. gigas*.

DNA methylation occurring in different genomic functional regions has different regulatory effects on gene expression. DNA methylation in promoter regions was often overlooked due to low levels of DNA methylation in invertebrates. However, studies have shown that DNA methylation of the *C. gigas* promoter has a function similar to that of vertebrate promoters and can regulate transcriptional activity (Saint-Carlier and Riviere 2015). However, in *Pinctada fucata martensii*, promoter DNA methylation was found to be positively correlated with gene expression except for the highly expressed genes (Zhang et al. 2020). In this study, we observed DNA methylation in the promoter regions but not all negatively regulated in gene expression. Therefore, we speculate that the repression of gene transcription by promoter DNA methylation may not be a general mechanism in mollusks. Further, a study had reported

Fig. 8 Gene-body, promoter DNA methylation with LncRNA expression. **a**, **b** Gene-body, promoter DNA methylation level with LncRNA expression level in CC strain. **c**, **d** Gene-body, promoter DNA methylation level with LncRNA expression level in HH strain
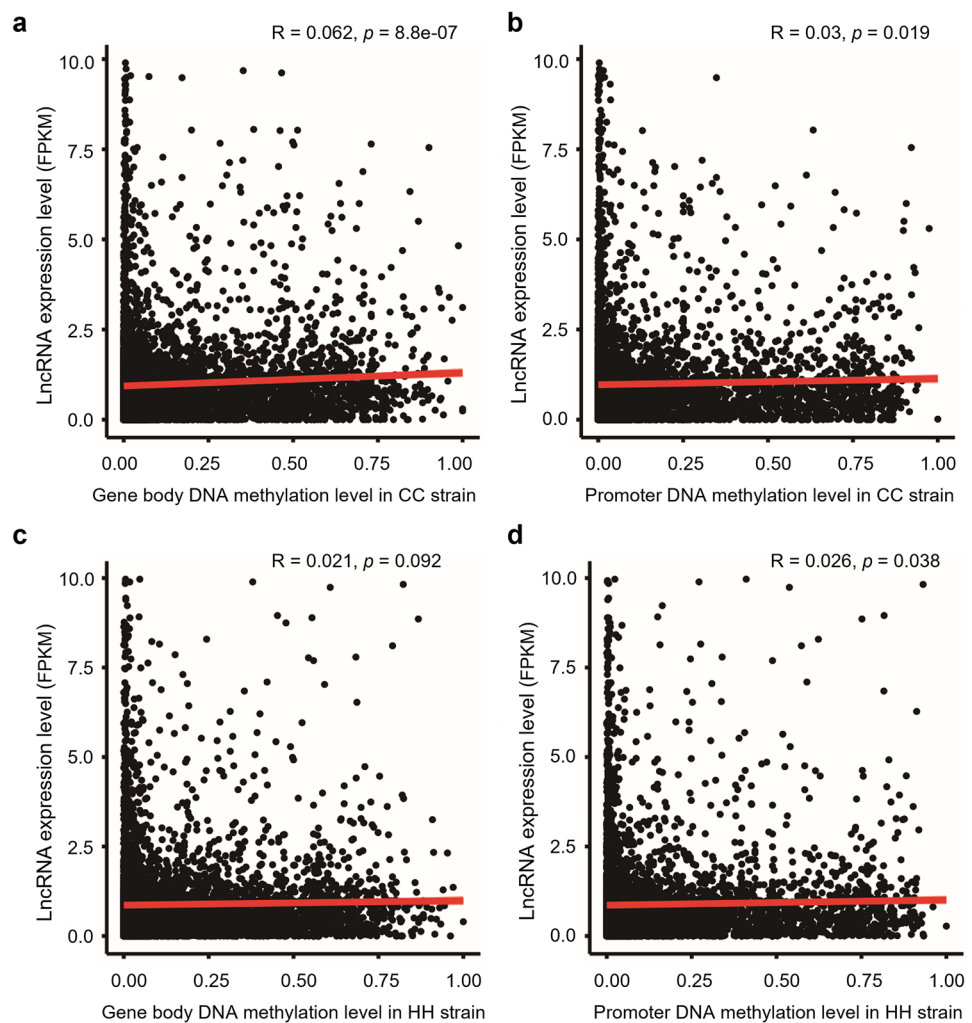
that DNA methylation occurring at specific locations in promoter regions could have an effect on gene expression, such as core transcription factor binding sites (Medvedeva et al. 2013). Through integrative analysis of DNA methylation and transcriptome analysis, we found that the DNA methylation in the gene body was positively correlated with gene expression in *C. gigas*. Genes showing higher levels of DNA methylation also had higher expression levels. This phenomenon was not only found in *C. gigas*, but also in mollusks such as *Biomphalaria glabrata* and *P. fucata martensii* (Gavery and Roberts 2013; Luviano et al. 2021; Wang et al. 2021; Zhang et al. 2020). The regulatory mechanism of gene expression by DNA methylation in the gene body can be variable and very complicated. Some studies reported that unmethylated exons were significantly shorter than methylated exons, while highly expressed exons usually have high levels of DNA methylation (Flores et al. 2012; Li et al. 2018; Song et al. 2017). Studies also suggested that DNA methylation in exons can mark the chromatin for modification, thereby reducing the chance of exon

skipping, which may lead to a higher rate of exon inclusion during transcription (Flores et al. 2012; Li et al. 2018). The involvement of DNA methylation in regulating alternative splicing has also been shown using dCas9 fused to enzymes that methylate or demethylate DNA (Shayevitch et al. 2018).

The relationship between DNA methylation and expression of genes is complex. In this study, we identified a total of 2133 DEGs that were differentially methylated, accounting for 27.42% of all DEGs. Among these 2133 genes, promoter DNA methylation or gene body DNA methylation did not show consistent correlation with gene expression. The transcriptional regulation of genes can be affected by many factors, such as DNA methylation, histone modifications, and availability of transcription factors (Gibney and Nolan 2010; van Breda et al. 2015). In addition, DNA methylation needs to occur at specific sites to have an effect on gene expression (Medvedeva et al. 2013). Therefore, the effects of the complex interaction of these factors on gene expression are difficult to predict.

We used DEGs to construct protein–protein interaction networks and perform association analysis with DNA

methylation. Within the network, the extracellular matrix (ECM) and integrin family genes were identified as the hub genes by the MCC method. As a major family of cell surface adhesion receptors, integrins can interact with ECM proteins and form cytoplasmic focal adhesions that are associated with the actin cytoskeleton (Wozniak et al. 2004). The ECM–integrin–actin cytoskeleton axis serves as a mechanical signal that can activate various downstream signaling pathways to regulate cell survival, proliferation, motility, differentiation, and cytoskeletal organization (Hynes 1992, 2002). FN1 can form a complex with integrin to regulate cell proliferation and enhance cell adhesion (Wirth et al. 2020). Highly expressed COL6A3 can promote the growth of mouse embryonic fibroblasts (MEFs) by inhibiting the Hippo signaling pathway and promoting the Wnt signaling pathway (Wang and Pan 2020). Furthermore, studies suggested that THBS1 induces cell cycle arrest through p53-mediated upregulation of p21 expression (Yamauchi et al. 2007). Interestingly, DNA methylation in promoter regions and expression of integrin beta-6 (LOC105346726) differed significantly between the CC and HH strains. The human homolog of the oyster integrin beta-6 was ITGB3, which was one of the cell surface receptors that mediate cell–matrix interactions, playing a variety of roles through binding to different ligands (De Arcangelis 2000; Moreno-Layseca et al. 2019; Zhu et al. 2019). It's reported that ITGB3 is a hub modulator of the PI3K/Akt signaling pathway involved in various growth-related processes, such as cell proliferation, and cell survival (Lei et al. 2011; Wan et al. 2019). Overexpression of ITGB3 could induce p53 pathway activation and the secretion of TGF-β to regulate cellular senescence (Rapisarda et al. 2017). Despite the highly diverse integrin family genes identified in many mollusk species (Dyachuk et al. 2015; Lv et al. 2020), we still have not fully understood the function of this versatile receptor family in invertebrates. We speculate that ECM-integrin signals might act as the crucial regulators of growth traits in the oyster. Furthermore, we show that integrin beta-6 (homolog of human ITGB3) is a hub modulator in regulating growth-related processes, which deserves future investigations.

Conclusion

In this work, we developed genome-wide DNA methylation profiles of two *C. gigas* strains with contrasted growth performance. Through comparative analysis, we identified a total of 339,604 differentially methylated CpG sites (DMCs) with were clustered into 27,600 differentially methylated regions (DMRs). Gene annotation identified a total of 11,033 genes from DMRs which were enriched in biological processes including cytoskeleton system, cell cycle, signal

transduction process, protein transcription, and translation. Integrative analysis of DNA methylation and transcriptome data revealed a positive correlation between gene expression and DNA methylation within the gene body. Protein–protein interaction analysis of differentially expressed and methylated genes allowed for the identification of ITGB3 as a hub modulator of the PI3K/Akt signaling pathway that was involved in various growth-related processes. This work provided insights into epigenetic regulation of growth in oysters and will be valuable resources for the study of DNA methylation in invertebrates.

Data Availability The datasets in this study have been submitted to the Sequence Read Archive (SRA) of the National Center for Biotechnology Information with the BioProject accession number PRJNA833956.

Declarations

References

Achrem M, Szućko I, Kalinka A (2020) The epigenetic regulation of centromeres and telomeres in plants and animals. Comp Cytogenet 14:265–311

Akalin A, Kormaksson M, Li S, Garrett-Bakelman FE, Figueroa ME, Melnick A, Mason CE (2012) methylKit: a comprehensive R package for the analysis of genome-wide DNA methylation profiles. Genome Biol 13:R87

Anastasiadi D, Esteve-Codina A, Piferrer F (2018) Consistent inverse correlation between DNA methylation of the first intron and gene expression across tissues and species. Epigenetics Chromatin 11:37

Azéma P, Lamy JB, Boudry P, Renault T, Travers MA, Dégremont L (2017) Genetic parameters of resistance to *Vibrio aestuarianus*, and OsHV-1 infections in the Pacific oyster, *Crassostrea gigas*, at three different life stages. Genet Sel Evol 49:23

Baylin SB, Jones PA (2016) Epigenetic determinants of cancer. Cold Spring Harb Perspect Biol 8:a019505

Bhatia G, Patterson N, Sankararaman S, Price AL (2013) Estimating and interpreting F ST : the impact of rare variants. Genome Res 23:1514–1521

Bolger AM, Lohse M, Usadel B (2014) Trimmomatic: a flexible trimmer for Illumina sequence data. Bioinformatics 30:2114–2120

Bouwland-Both MI, van Mil NH, Stolk L, Eilers PHC, Verbiest MMPJ, Heijmans BT, Tiemeier H, Hofman A, Steegers EAP, Jaddoe VWV, Steegers-Theunissen RPM (2013) DNA methylation of IGF2DMR and H19 is associated with fetal and infant growth: the Generation R Study. PLoS ONE 8:e81731

Brown J, Pirrung M, McCue LA (2017) FQC dashboard: integrates FastQC results into a web-based, interactive, and extensible FASTQ quality control tool. Bioinformatics 33:3137–3139

Chin C-H, Chen S-H, Wu H-H, Ho C-W, Ko M-T, Lin C-Y (2014) cyto-Hubba: identifying hub objects and sub-networks from complex interactome. BMC Syst Biol 8:S11

Cohen CJ, Lock WM, Mager DL (2009) Endogenous retroviral LTRs as promoters for human genes: a critical assessment. Gene 448:105–114

De Arcangelis A (2000) Integrin and ECM functions: roles in vertebrate development. Trends Genet 16:389–395

de Melo CMR, Durland E, Langdon C (2016) Improvements in desirable traits of the Pacific oyster, *Crassostrea gigas*, as a result of five generations of selection on the West Coast, USA. Aquaculture 460:105–115

Dupont C, Armant D, Brenner C (2009) Epigenetics: definition, mechanisms and clinical perspective. Seminars in Reproductive Medicine 27:351–357

Dyachuk VA, Maiorova MA, Odintsova NA (2015) Identification of *β* integrin-like- and fibronectin-like proteins in the bivalve mollusk *Mytilus trossulus*. Dev Growth Differ 57:515–528

Esteller M (2005) DNA methylation: approaches, methods, and applications. CRC Press, Boca Raton

Evans S, Langdon C (2006) Direct and indirect responses to selection on individual body weight in the Pacific oyster (*Crassostrea gigas*). Aquaculture 261:546–555

Fan Y, Liang Y, Deng K, Zhang Z, Zhang G, Zhang Y, Wang F (2020) Analysis of DNA methylation profiles during sheep skeletal muscle development using whole-genome bisulfite sequencing. BMC Genomics 21:327

Flores K, Wolschin F, Corneveaux JJ, Allen AN, Huentelman MJ, Amdam GV (2012) Genome-wide association between DNA methylation and alternative splicing in an invertebrate. BMC Genomics 13:480

Gavery MR, Roberts SB (2013) Predominant intragenic methylation is associated with gene expression characteristics in a bivalve mollusc. PeerJ 1:e215

Gavery MR, Roberts SB (2010) DNA methylation patterns provide insight into epigenetic regulation in the Pacific oyster (*Crassostrea gigas*). BMC Genomics 11:483

Gibney ER, Nolan CM (2010) Epigenetics and gene expression. Heredity 105:4–13

Guo W, Zhu P, Pellegrini M, Zhang MQ, Wang X, Ni Z (2018) CGmapTools improves the precision of heterozygous SNV calls and supports allele-specific methylation detection and visualization in bisulfite-sequencing data. Bioinformatics 34:381–387

Guo XM (2009) Use and exchange of genetic resources in molluscan aquaculture: genetic resources in molluscan aquaculture. Rev Aquac 1:251–259

Gutierrez AP, Matika O, Bean TP, Houston RD (2018) Genomic selection for growth traits in Pacific oyster (*Crassostrea gigas*): potential of low-density marker panels for breeding value prediction. Front Genet 9:391

Han Z, Li Q, Xu C, Liu S, Yu H, Kong L (2021) QTL mapping for orange shell color and sex in the Pacific oyster (*Crassostrea gigas*). Aquaculture 530:735781

Hao Z, Lv D, Ge Y, Shi J, Weijers D, Yu G, Chen J (2020) *RIdeogram*: drawing SVG graphics to visualize and map genome-wide data on the idiograms. PeerJ Computer Science 6:e251

He X, Li C, Qi H, Meng J, Wang W, Wu F, Li L, Zhang G (2021) A genome-wide association study to identify the genes associated with shell growth and shape-related traits in *Crassostrea gigas*. Aquaculture 543:736926

Hu B, Tian Y, Li Q, Liu S (2021) Genomic signatures of artificial selection in the Pacific oyster, *Crassostrea gigas*. Evol Appl 00:1–13

Hu T, Zhu X, Pi W, Yu M, Shi H, Tuan D (2017) Hypermethylated LTR retrotransposon exhibits enhancer activity. Epigenetics 12:226–237

Hu Y, Xu H, Li Z, Zheng X, Jia X, Nie Q, Zhang X (2013) Comparison of the genome-wide DNA methylation profiles between fast-growing and slow-growing broilers. PLoS ONE 8:e56411

Hynes RO (1992) Integrins: versatility, modulation, and signaling in cell adhesion. Cell 69:11–25

Hynes RO (2002) Integrins: bidirectional, allosteric signaling machines. Cell 110:673–687

Jiao Z, Tian Y, Hu B, Li Q, Liu S (2021) Genome structural variation landscape and its selection signatures in the fast-growing strains of the Pacific oyster, *Crassostrea gigas*. Mar Biotechnol 23:736–748.

Julicher F, Kruse K, Prost J, Joanny J (2007) Active behavior of the cytoskeleton. Phys Rep 449:3–28

Kim EY, Choi YH (2019) Regulation of adductor muscle growth by the IGF-1/AKT pathway in the triploid Pacific oyster. Crassostrea Gigas Fisheries and Aquatic Sciences 22:19

Krauss G (2003) Biochemistry of signal transduction and regulation. Wiley-VCH, Weinheim

Lei Y, Huang K, Gao C, Lau QC, Pan H, Xie K, Li J, Liu R, Zhang T, Xie N, Nai HS, Wu H, Dong Q, Zhao X, Nice EC, Huang C, Wei Y (2011) Proteomics identification of ITGB3 as a key regulator in reactive oxygen species-induced migration and invasion of colorectal cancer cells. Mol Cell Proteomics 10:005397

Li Q, Wang Q, Liu S, Kong L (2011) Selection response and realized heritability for growth in three stocks of the Pacific oyster *Crassostrea gigas*. Fish Sci 77:643–648

Li Q, Yu H, Yu R (2006) Genetic variability assessed by microsatellites in cultured populations of the Pacific oyster (*Crassostrea gigas*) in China. Aquaculture 259:95–102

Li S, Zhang J, Huang S, He X (2018) Genome-wide analysis reveals that exon methylation facilitates its selective usage in the human transcriptome. Brief Bioinform 19:754–764

Li Y, Ren L, Fu H, Yang B, Tian J, Li Q, Liu Z, Liu S (2021) Crosstalk between dopamine and insulin signaling in growth control of the oyster. Gen Comp Endocrinol 313:113895

Liew YJ, Howells EJ, Wang X, Michell CT, Burt JA, Idaghdour Y, Aranda M (2020) Intergenerational epigenetic inheritance in reef-building corals. Nat Clim Chang 10:254–259

Luviano N, Lopez M, Gawehns F, Chaparro C, Arimondo PB, Ivanovic S, David P, Verhoeven K, Cosseau C, Grunau C (2021) The methylome of *Biomphalaria glabrata* and other mollusks: enduring modification of epigenetic landscape and phenotypic traits by a new DNA methylation inhibitor. Epigenetics Chromatin 14:48

Lv Z, Qiu L, Wang W, Liu Z, Liu Q, Wang L, Song L (2020) The members of the highly diverse *Crassostrea gigas* integrin family cooperate for the generation of various immune responses. Front Immunol 11:1420

Lyko F, Foret S, Kucharski R, Wolf S, Falckenhayn C, Maleszka R (2010) The honey bee epigenomes: differential methylation of brain DNA in queens and workers. PLoS Biol 8:e1000506

Ma X, Jia C, Chu M, Fu D, Lei Q, Ding X, Wu X, Guo X, Pei J, Bao P, Yan P, Liang C (2019) Transcriptome and DNA methylation analyses of the molecular mechanisms underlying with longissimus dorsi muscles at different stages of development in the polled yak. Genes 10:970

Männer L, Schell T, Provataris P, Haase M, Greve C (2021) Inference of DNA methylation patterns in molluscs. Philos Trans R Soc B 376:20200166

Medvedeva YA, Khamis AM, Kulakovskiy IV, Ba-Alawi W, Bhuyan SI, Kawaji H, Lassmann T, Harbers M, Forrest AR, Bajic VB (2013) Effects of cytosine methylation on transcription factor binding sites. BMC Genomics 15:119

Moore LD, Le T, Fan G (2013) DNA Methylation and its basic function. Neuropsychopharmacology 38:23–38

Moreno-Layseca P, Icha J, Hamidi H, Ivaska J (2019) Integrin trafficking in cells and tissues. Nat Cell Biol 21:122–132

Pappalardo XG, Barra V (2021) Losing DNA methylation at repetitive elements and breaking bad. Epigenetics Chromatin 14:25

Park JS, Burckhardt CJ, Lazcano R, Solis LM, Isogai T, Li L, Chen CS, Gao B, Minna JD, Bachoo R, DeBerardinis RJ, Danuser G (2020) Mechanical regulation of glycolysis via cytoskeleton architecture. Nature 578:621–626

Pucci B, Kasten M, Giordano A (2000) Cell cycle and apoptosis. Neoplasia 2:291–299

Rapisarda V, Borghesan M, Miguela V, Encheva V, Snijders AP, Lujambio A, O'Loghlen A (2017) Integrin beta 3 regulates cellular senescence by activating the TGF-β pathway. Cell Rep 18:2480–2493

Roberts SB, Gavery MR (2012) Is there a relationship between DNA methylation and phenotypic plasticity in invertebrates? Front Physiol 2:116

Saint-Carlier E, Riviere G (2015) Regulation of Hox orthologues in the oyster Crassostrea gigas evidences a functional role for promoter DNA methylation in an invertebrate. FEBS Lett 589:1459–1466

Šatović Vukšić E, Plohl M (2021) Exploring satellite DNAs: specificities of bivalve mollusks genomes. In: Ugarković Đ (eds) Satellite DNAs in physiology and evolution. Prog Mole Subcell Biol vol 60. Springer, Cham

Scelfo A, Fachinetti D (2019) Keeping the centromere under control: a promising role for DNA methylation. Cells 8:912

Shayevitch R, Askayo D, Keydar I, Ast G (2018) The importance of DNA methylation of exons on alternative splicing. RNA 24:1351–1362

Shi C, Zhang F, Li Q, Liu S (2022) Gene expression signatures underlying inbreeding depression as revealed by whole-transcriptome analysis of selectively bred strains of the Pacific Oyster (Crassostrea gigas). bioRxiv/2022/490184

Song K, Li L, Zhang G (2017) The association between DNA methylation and exon expression in the Pacific oyster Crassostrea gigas. PLoS ONE 12:e0185224

Sun D, Xi Y, Rodriguez B, Park HJ, Tong P, Meong M, Goodell MA, Li W (2014) MOABS: model based analysis of bisulfite sequencing data. Genome Biol 15:R38

Suzuki MM, Kerr ARW, De Sousa D, Bird A (2007) CpG methylation is targeted to transcription units in an invertebrate genome. Genome Res 17:625–631

Troost K (2010) Causes and effects of a highly successful marine invasion: case-study of the introduced Pacific oyster Crassostrea gigas in continental NW European estuaries. J Sea Res 64:145–165

Tunjić-Cvitanić M, Pasantes JJ, García-Souto D, Cvitanić T, Plohl M, Šatović-Vukšić E (2021) Satellitome analysis of the Pacific oyster Crassostrea gigas reveals new pattern of satellite DNA organization, highly scattered across the genome. Int J Mol Sci 22:6798

van Breda SGJ, Claessen SMH, Lo K, van Herwijnen M, Brauers KJJ, Lisanti S, Theunissen DHJ, Jennen DGJ, Gaj S, de Kok TMCM, Kleinjans JCS (2015) Epigenetic mechanisms underlying arsenic-associated lung carcinogenesis. Arch Toxicol 89:1959–1969

Vergeer P, Wagemaker N, Ouborg NJ (2012) Evidence for an epigenetic role in inbreeding depression. Biol Let 8:798–801

Vermeulen K, Berneman ZN, Van Bockstaele DR (2003) Cell cycle and apoptosis. Cell Prolif 36:165–175

Wan H, Xie T, Xu Q, Hu X, Xing S, Yang H, Gao Y, He Z (2019) Thy-1 depletion and integrin β3 upregulation-mediated PI3K-Akt-mTOR pathway activation inhibits lung fibroblast autophagy in lipopolysaccharide-induced pulmonary fibrosis. Lab Invest 99:1636–1649

Wang J (2018) An integrated genetic map based on EST-SNPs and QTL analysis of shell color traits in Pacific oyster Crassostrea gigas. Aquaculture 429:226–236

Wang J, Pan W (2020) The biological role of the collagen alpha-3 (VI) chain and its cleaved C5 domain fragment endotrophin in cancer. Onco Targets Ther 13:5779–5793

Wang Q (2013) Tagmentation-based whole-genome bisulfite sequencing. Nat Protoc 8:2022–2032

Wang X, Li A, Wang W, Que H, Zhang G, Li L (2021) DNA methylation mediates differentiation in thermal responses of Pacific oyster (Crassostrea gigas) derived from different tidal levels. Heredity 126:10–22

Wells JN, Feschotte C (2020) A field guide to eukaryotic transposable elements. Annu Rev Genet 54:539–561

Wickstead B, Gull K (2011) The evolution of the cytoskeleton. J Cell Biol 194:513–525

Wirth F, Lubosch A, Hamelmann S, Nakchbandi IA (2020) Fibronectin and its receptors in hematopoiesis. Cells 9:2717

Wozniak MA, Modzelewska K, Kwong L, Keely PJ (2004) Focal adhesion regulation of cell behavior. Biochim. Biophys. Biochimica et Biophysica Acta (BBA) - Mole Cell Res 1692:103–119

Xi Y, Li W (2009) BSMAP: whole genome bisulfite sequence mapping program. BMC Bioinformatics 10:232

Yamauchi M, Imajoh-Ohmi S, Shibuya M (2007) Novel antiangiogenic pathway of thrombospondin-1 mediated by suppression of the cell cycle. Cancer Sci 98:1491–1497

Yang Y, Liang G, Niu G, Zhang Y, Zhou R, Wang Y, Mu Y, Tang Z, Li K (2017) Comparative analysis of DNA methylome and transcriptome of skeletal muscle in lean-, obese-, and mini-type pigs. Sci Rep 7:39883

Yu, G, Wang LG, Han Y, He QY (2012) clusterProfiler: an R package for comparing biological themes among gene clusters. OMICS: J Integ Biol 16:284–287

Zhang F, Hu B, Fu H, Jiao Z, Li Q, Liu S (2019) Comparative transcriptome analysis reveals molecular basis underlying fast growth of the selectively bred Pacific oyster. Crassostrea Gigas Frontiers in Genetics 10:610

Zhang J, Luo S, Gu Z, Deng Y, Jiao Y (2020) Genome-wide DNA Methylation analysis of mantle edge and mantle central from pearl oyster Pinctada fucata martensii. Mar Biotechnol 22:380–390

Zhu C, Kong Z, Wang B, Cheng W, Wu A, Meng X (2019) ITGB3/CD61: a hub modulator and target in the tumor microenvironment. Am J Transl Res 11:7195–7208